

Excited-state density distributions in neutron-rich nuclei

J. Terasaki

*Department of Physics and Astronomy, University of North Carolina, Chapel Hill, North Carolina 27599-3255, USA and
School of Physics, Peking University, Beijing 100871, People's Republic of China*

J. Engel

Department of Physics and Astronomy, University of North Carolina, Chapel Hill, North Carolina 27599-3255, USA

(Received 31 July 2006; published 23 October 2007)

We calculate densities of excited states in the quasiparticle random-phase approximation (QRPA) with Skyrme interactions and volume pairing. We focus on low-energy peaks/bumps in the strength functions of a range of Ca, Ni, and Sn isotopes for $J^\pi = 0^+$, 1^- , and 2^+ . We define an “emitted-neutron number,” which we then use to distinguish localized states from scattering-like states. The degree of delocalization either increases as the neutron-drip line is approached or stays high between the stability line and the drip line. In the 2^+ channel of Sn, however, the low-lying states, not even counting surface vibrations, are still fairly well localized on average, even at the neutron drip line.

DOI: [10.1103/PhysRevC.76.044320](https://doi.org/10.1103/PhysRevC.76.044320)

PACS number(s): 21.10.Pc, 21.60.Jz, 27.50.+e, 27.60.+j

I. INTRODUCTION

The structure of excited states in exotic nuclei has been much studied recently, both in nuclei between Li and O [1–4] and in heavier Ca [5] and Sn [6] isotopes. Low-energy strength in neutron-rich nuclei is often enhanced, and theorists have tried to understand the mechanisms responsible, particularly in the isovector $J^\pi = 1^-$ channel, where the low-energy peak is often referred to as a “pygmy resonance” because the enhancement, though significant, does not make the peak as large as the higher-energy giant resonance. Many articles have used the random-phase approximation (RPA) or its extension, the quasiparticle random-phase approximation (QRPA), to predict the existence of a pygmy in spherical medium-heavy nuclei (see Refs. [7–12] and references therein) with qualitatively similar results.¹ Following the initial work of Ref. [8] on certain 0^+ states, theorists now seem in agreement that a “threshold effect,” corresponding to the significant overlap of bound but spatially extended single-neutron orbitals with low-lying continuum orbitals, is responsible for the low-energy enhancement near the neutron-drip line. Reference [16] discusses a “soft-dipole” mechanism in which protons in the nucleus oscillate collectively against the spatially extended neutron matter. This soft mode, while present in many nuclei, becomes less important for the strength as the neutron-drip line is approached.

Many of the articles cited above calculate the spatial distribution of transition strength, known as the “transition density.” This observable has the distinct advantage that it has been measured for low-lying states and giant resonances in a number of nuclei and is measurable in principle even away from stability. References [9,12], for example, use calculated transition densities to argue that although protons inside the nucleus contribute to the pygmy resonance, a long neutron

tail is the direct origin for the enhancement of the transition strength. We have recently investigated [12] strength functions and transition densities in a large range of medium-heavy spherical nuclei, from one drip line to the other, finding that pygmylike states exist not only in the isovector dipole channel but also elsewhere.²

Transition densities tell us about where in the nucleus transitions occur; they reflect the spatial distribution of products of single-particle and single-hole wave functions and, as a consequence, are always localized, though they can be very extended near the neutron drip line. In nuclei near stability large transition strength implies collectivity, which in turn tends to cause localization (as we shall see in giant resonances). Near the drip line, however, the familiar relations among strength, collectivity, and localization are less systematic at low energies. As Ref. [12] shows, the threshold effect that characterizes light halo nuclei, i.e., large strength coming from noncollective transitions to very spatially extended single-particle states, manifests itself quite generally in low-lying peaks. The excited single-particle states are often unbound and may not even be quasibound; that is, they may be completely delocalized scattering states [8]. We need to look beyond measures of collectivity, beyond necessarily localized transition densities, if we want to understand the degree to which the excited states themselves are localized.

In this article we suggest a measure of localization and then investigate the extent to which the strong low-lying excited states are localized, independent of their collectivity. To uncover changes in structure near the drip line, we track the degree of localization as N increases in $J^\pi = 0^+$, 1^- , and 2^+ channels. Localization, which we analyze by examining *diagonal* density distributions of the excited states, has not been systematically studied before and offers a new window into excitations in exotic neutron-rich nuclei.

¹The importance of correlations beyond QRPA to the pygmy is still an open issue [10,13–15].

²The degree of enhancement varies significantly with the channel.

II. MEASURE OF LOCALIZATION

We can adopt ideas from simple one-particle quantum mechanics to distinguish localized states from extended ones. If the energy of a single particle in, e.g., a square-well potential is negative (Ch. 3 of Ref. [17]), then the tail of its wave function decays exponentially, and if the energy is positive the tail oscillates. In certain small positive-energy windows, however, the amplitude of the oscillating tail is much smaller than that of the wave function inside the potential. Such states are sometimes called “quasibound,” and the solutions that exhibit no enhancement inside are sometimes referred to as “scattering states.”

Of course, we are dealing with many-body quantum mechanics and the asymptotic wave function depends on many coordinates. The tail of the one-body density, however, should still give us a measure of localization. Here we use the Skyrme-QRPA wave functions (with the parameter set SkM* and volume pairing) from Ref. [12], in which we discussed transition densities, to obtain the diagonal density of excited-state k :

$$\begin{aligned} \rho_k^q(\mathbf{r}) &= \langle k | \hat{\rho}_q(\mathbf{r}) | k \rangle \\ &= \sum_{KK'L} (-\psi_K^*(\mathbf{r})\psi_{K'}(\mathbf{r})u_K u_{K'} \\ &\quad + \psi_{\bar{K}}^*(\mathbf{r})\psi_{\bar{K}'}(\mathbf{r})v_{\bar{K}} v_{\bar{K}'}) \\ &\quad \times (X_{LK'}^k X_{KL}^k + Y_{KL}^k Y_{LK'}^k) + \rho_0^q(\mathbf{r}), \end{aligned} \quad (1)$$

where q takes values “proton” or “neutron,” $\hat{\rho}_q(\mathbf{r})$ is the corresponding density operator [and $\rho_0^q(\mathbf{r})$ the corresponding ground-state density], $\psi_K(\mathbf{r})$ is a single-particle wave function in the canonical basis, and u_K and v_K are the associated occupation amplitudes. The QRPA amplitudes $X_{KK'}^k$ and $Y_{KK'}^k$ are assumed real, \bar{K} denotes the state conjugate to K , and we have used the convention $\psi_{\bar{K}}(\mathbf{r}) = -\psi_K(\mathbf{r})$. The sums run over either proton or neutron states, not both. Equation (1) can be derived from

$$\langle 0 | O_k \hat{\rho}(\mathbf{r}) O_k^\dagger | 0 \rangle = \langle 0 | [O_k, [\hat{\rho}(\mathbf{r}), O_k^\dagger]] + [O_k, O_k^\dagger] \hat{\rho}(\mathbf{r}) | 0 \rangle, \quad (2)$$

where $|0\rangle$ is the correlated ground state, and

$$|k\rangle = O_k^\dagger |0\rangle, \quad O_k |0\rangle = 0, \quad (3)$$

$$O_k^\dagger = \frac{1}{2} \sum_{KK'} (X_{KK'}^k a_K^\dagger a_{K'}^\dagger - Y_{KK'}^k a_{K'} a_K), \quad (4)$$

$$X_{K'K}^k = -X_{KK'}^k, \quad Y_{K'K}^k = -Y_{KK'}^k, \quad K < K', \quad (5)$$

where a_K^\dagger and a_K are the creation and annihilation operators for quasiparticles in the canonical state K . The effects of ground-state correlations on the excited-state densities appear in the Y terms in Eq. (1).

If, as in all the calculations presented here, the ground state is spherically symmetric, the number of type- q particles between two radii is just the integral over that well-defined region of $\rho_k^q(r)r^2$. We define the “emitted-neutron number” associated with the state k as

$$N_e(k) = 4\pi \int_{r \geq r_c} dr r^2 [\rho_k^n(r) - \rho_0^n(r)], \quad (6)$$

where r_c denotes the radius at which the density $\rho_k^n(r)$ begins to develop a scattering tail. The point of the definition is to count the number of neutrons in this excited-state tail. In addition to the tail, the excited-state density contains an exponentially falling piece that cannot be isolated and subtracted without some sort of extrapolation/prescription. Here we assume that the exponentially falling piece is the same as that of the ground state,³ which has no scattering tail. Any other sensible prescription would give similar results because the falling piece contributes so little beyond r_c . Another definition of emitted particle number for the ionization of metal clusters is proposed in Ref. [18]. If the excitation is a single particle-hole, that definition is almost equivalent to ours.

If $N_e(k)$ is close to or larger than 1, then the excited state is scattering-like (not localized), and if $N_e(k)$ is appreciably smaller than 1, then the excited state qualifies as quasibound (localized). Intermediate cases are also possible, of course. If the pairing gap is not zero $\rho_k^n(r)$ does not integrate to the correct particle number.⁴ But because the error comes from the pairing correlations, the quasiparticle states responsible for the error are near the Fermi surface, and the wave functions are confined within the nucleus and do not contribute significantly to $N_e(k)$. We therefore multiply $\rho_k^n(r)$ by a constant—at most a few percentages from unity—to normalize it correctly. This resulting error in $N_e(k)$ is also at most a few percentages and will not affect our conclusions. We return to this point in more detail later.

Rather than focus on individual states, we want to examine peaks in the strength function, which can encompass several discrete states. Some of those discrete states may not be entirely representative of the average behavior of the resonance. We therefore define a strength-weighted average of the emitted-neutron number for the strongly excited states k within a given peak:

$$\bar{N}_e = \frac{1}{2} (\bar{N}_e^{\text{IS}} + \bar{N}_e^{\text{IV}}), \quad (7)$$

$$\bar{N}_e^{\text{IS}} = \frac{\sum_k S_k^{\text{IS}} N_e(k)}{\sum_k S_k^{\text{IS}}}, \quad \bar{N}_e^{\text{IV}} = \frac{\sum_k S_k^{\text{IV}} N_e(k)}{\sum_k S_k^{\text{IV}}}, \quad (8)$$

where S_k^{IS} and S_k^{IV} denote isoscalar and isovector transition strengths to the state k . The number of terms in the sums is between 1 and 10. We average the isoscalar and isovector quantities because both channels appear in low-energy strength-function peaks, particularly near the drip line. The giant resonances do not have this property, however, and for them we will use \bar{N}_e^{IS} or \bar{N}_e^{IV} as measures.

Before investigating the dependence of emitted-neutron number on N and Z , we need to see whether we can calculate it reliably. The tail of the nuclear density is extraordinarily sensitive and converges slowly both with the size of our spatial “box” and the number of canonical states in our basis. Figure 1 shows the isoscalar 0^+ strength distribution for ^{50}Ca

³We estimate the maximum possible error due to a halo to be around 0.2 near the neutron drip line of Ca. Heavier isotopes seem not to have halos.

⁴The QRPA does not guarantee the conservation of a quantity that is of second order or higher in the X 's and Y 's.

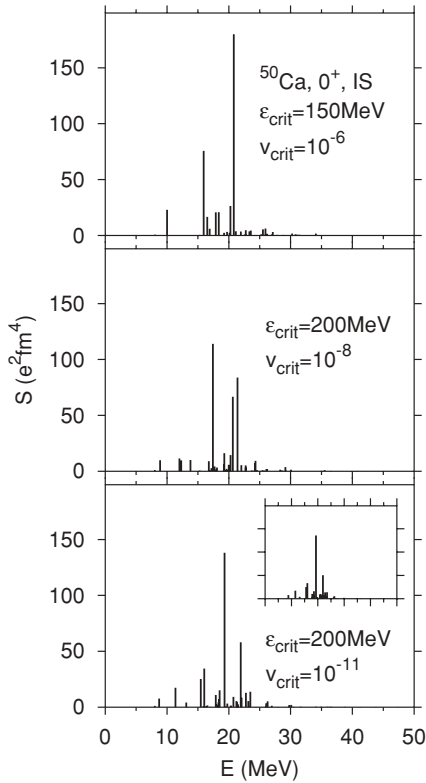


FIG. 1. Strength distributions in the isoscalar 0^+ channel of ^{50}Ca , with a box size 20 fm. The neutron chemical potential is -6.61 MeV. The inset in the bottom panel corresponds to a calculation with $\epsilon_{\text{crit}} = 250$ MeV and $\nu_{\text{crit}} = 10^{-14}$ and has the same scale as the other graphs.

in a few versions of our calculation. We have varied two cutoff parameters: an upper limit ϵ_{crit} on canonical single-particle energies (for protons, which have a vanishing pairing gap), and a lower limit ν_{crit} on occupation amplitudes (for neutrons, which have a nonvanishing gap). We confirmed, and the inset shows, that when $\epsilon_{\text{crit}} = 250$ MeV and $\nu_{\text{crit}} = 10^{-14}$, the strength distribution is almost identical to that with $\epsilon_{\text{crit}} = 200$ MeV and $\nu_{\text{crit}} = 10^{-11}$. In Refs. [12,19] we folded the strength to account for the 20-fm box radius, and the values $\epsilon_{\text{crit}} = 150$ MeV and $\nu_{\text{crit}} = 10^{-6}$ were sufficient for convergence of the strength function and transition densities to the level of accuracy we required. Figure 1 seems to suggest, however, that larger spaces are required to reproduce the tiny part of the excited-state density that lies significantly outside the nucleus.

To examine the issue more closely, we show in Fig. 2 the neutron density distribution associated with a low-lying state in the top part of Fig. 1; that distribution was obtained with the cutoff parameters we used extensively in Ref. [12]. In Fig. 3 we show the neutron densities associated with the corresponding states in the bottom part of Fig. 1, obtained in a larger space. The tails of the more accurate densities are noticeably different (and more realistic). Yet improving the description this way has a relatively small effect on the emitted-neutron number. In the smaller space the \bar{N}_e of low-energy states is 0.84, with individual $N_e(k)$ ranging from

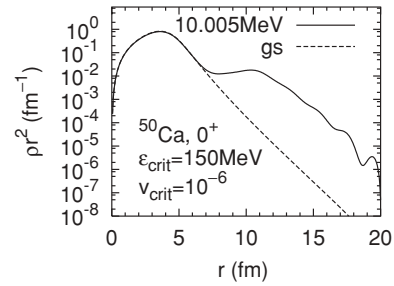


FIG. 2. Neutron-density distribution of the low-energy state with non-negligible strength in ^{50}Ca (see Fig. 1), calculated with $\epsilon_{\text{crit}} = 150$ MeV, $\nu_{\text{crit}} = 10^{-6}$, and a box radius of 20 fm. The excitation energy is at the top of the figure. The ground-state (gs) density obtained in the Hartree-Fock-Bogoliubov approximation is also drawn. For this excited state $r_c = 7$ fm.

0.77 to 0.90, and in the larger space it is 0.89, with $N_e(k)$ ranging from 0.85 to 0.92. These ranges, 10% or less of the average, are not only small but also typical of cases with \bar{N}_e near 1. Changing the box radius to 25 fm fragments the strength by adding new states so that the $N_e(k)$ cannot really be tracked as the box size changes. The average \bar{N}_e over the states in a certain energy range, however, turns out not to change substantially; with a box size of 25 fm, \bar{N}_e is 0.86 for five sample states.⁵ We have used the 25-fm box for a few other states with different multipolarity and, as we show later, find similar levels of change. Perhaps the stability of \bar{N}_e , an integrated quantity, is not so surprising given that the smaller space is large enough to describe the wave functions extremely well for r less than r_c , so that the number of particles outside r_c is likewise well represented. In any event, we can conclude here—for the 0^+ bump below the giant resonance in ^{50}Ca —that the states are scattering-like. Nearly a full neutron is far outside the nucleus, no matter how we vary parameters.

⁵That is fortunate because 20 fm is the maximum radius we can use for systematic calculations across a range of isotopes.

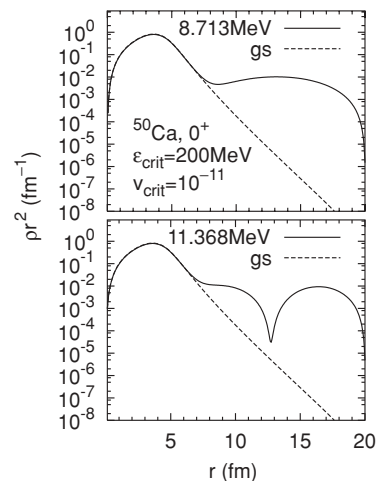


FIG. 3. The same as Fig. 2 but for $\epsilon_{\text{crit}} = 200$ MeV and $\nu_{\text{crit}} = 10^{-11}$.

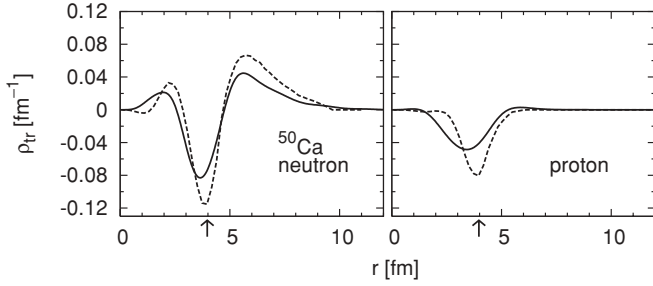


FIG. 4. Transition densities for the most significant state in the dipole pygmy resonance peak of ^{50}Ca , in our calculation (solid curve) and that of Matsuo *et al.* [20] (dashed curve). The energy of the excited state is $E = 9.4$ MeV in our calculation and 7.9 MeV in that of Ref. [20]. The arrow at the bottom horizontal line is a neutron radius at half-density of our calculation. The transition densities are normalized in such a way that the $B(E1) \uparrow$ obtained by integrating these curves gives the total transition strength in $0 < E < 10$ MeV.

As promised above, we return to the issue of particle-number nonconservation in a bit more detail. An important two-quasiparticle configuration in the excitation of Fig. 2 consists of one neutron quasiparticle in the $2p_{3/2}$ state and one in the $3p_{3/2}$ state. The $2p_{3/2}$ state causes an error in the particle number because its occupation number is nearly 0.5. (The other state is far above the Fermi surface.) But only 3% of its squared (canonical-basis) wave function is at $r > r_c = 7$ fm. The renormalization we introduced earlier to account for particle-number violation therefore has very little effect on $N_e(k)$.

One may wonder, despite the robustness of \bar{N}_e , whether our box-QRPA adequately represents the continuum. We can address the question by comparing our results with those of a continuum Green's function QRPA calculation. Figure 4 shows transition densities at the peak of the 1^- pygmy resonance in ^{50}Ca , calculated in the continuum QRPA by Matsuo *et al.* [20] and in the box-QRPA by us. The former calculation uses a Woods-Saxon potential and δ interaction, simpler than Skyrme interaction, in the particle-hole channel, while treating pairing correlations self-consistently with a surface-type δ interaction. Our calculation is self-consistent in both particle-hole and pairing channels. The similarity in the shapes of the two densities (if not the heights, which reflect different predictions for the total strength in the pygmy) given the difference in interactions and boundary conditions, is noteworthy, and supports the validity of our representation of wave functions outside the nucleus.

III. RESULTS AND DISCUSSION

To set a benchmark of sorts, we have looked at densities for giant resonances in the isoscalar and isovector 0^+ , 1^- , and 2^+ channels of several Ca, Ni, and Sn isotopes near stability. \bar{N}_e^{IS} and \bar{N}_e^{IV} are always on the order of 0.5 or less. The isoscalar giant dipole resonances have the largest values. The smallest belongs to the isovector giant quadrupole resonance of ^{58}Ni , with $\bar{N}_e^{\text{IS}} = 0.01$. The reasons for this very small value are that the main components of the neutron excitation involve deep

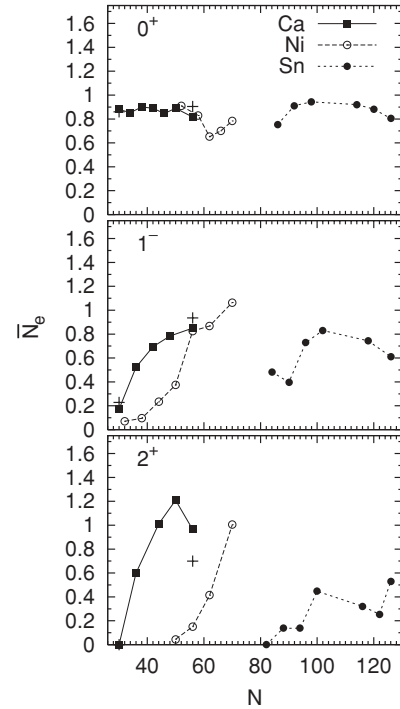


FIG. 5. \bar{N}_e in low-lying strength-function peaks, versus neutron number N , for the 0^+ , 1^- , and 2^+ channels of a sequence of Ca, Ni, and Sn isotopes. In the 2^+ channel, the lowest-energy states (surface vibrations), carrying the largest strengths, are not included. In Ni the 1^- curve has more points than those of the other J^π channels because the low-energy bump first appears at smaller N . Crosses show \bar{N}_e from calculations with a box of radius 25 fm. The results in the 0^+ and 2^+ channels of ^{50}Ca coincide almost exactly with those of the 20-fm box calculations.

hole states and particle states near the Fermi surface and that protons contribute appreciably.

Having established a good measure of localization and calibrated it for typical collective resonances, we are now in a position to examine the behavior of low-lying excitations in neutron-rich nuclei. In each channel we look at low-energy bumps in a range of Ca, Ni, and Sn isotopes. The resulting \bar{N}_e , plotted versus neutron number N , appear in Fig. 5. For 0^+ states they are more or less constant, at least in Ca and Sn, and because the constant is greater than 0.8, the wave functions in the bumps are not localized. The \bar{N}_e in the 1^- channel in Ca and Ni show a clear increase with N , from 0.1 to about 1; those states are localized near stability and become more scattering-like toward the drip line. The 1^- states in Sn are harder to interpret; the curve has a maximum of about 0.8 around $N = 100$, but shows no clear trend in one direction or the other. The 2^+ states in Ca and Ni mirror the behavior of the 1^- states. In the 2^+ channel of Sn, \bar{N}_e increases with N but the low-lying states never get less localized than typical giant resonances. By our criterion, those states are localized, on average, even at the drip line, though they fluctuate within a given peak in a way that cannot be seen in the average (some individual states have $N_e(k) > 0.8$). We should note that the states used to determine \bar{N}_e do not include low-lying surface quadrupole vibrations, which usually have $N_e(k) < 0.1$.

The crosses in Fig. 5 label results for ^{50}Ca and ^{76}Ca in a box of radius 25 fm. The results do not change qualitatively and in ^{50}Ca are essentially invisible, although in the 2^+ channel of ^{76}Ca the change is non-negligible. We did not extend these calculations to other nuclei because they are very CPU and memory intensive.

In Ref. [12] we found that the strength to low-lying bumps grew with N in essentially every channel and every isotopic chain. Though we sometimes see similar behavior in \bar{N}_e , it is not universal. The 0^+ states, for instance, are not localized even near stability. And the 2^+ states in Sn, although they become more scattering-like with increasing N , do not always delocalize beyond the level of giant resonances. All this comes with a caveat, however: it is possible that many-particle many-hole states that admix with QRPA excitations can alter \bar{N}_e somewhat. The one-particle one-hole nature of our states means, for instance, that \bar{N}_e is never much greater than 1. Calculating the structure of many-particle many-hole states is difficult, however, and it may be some

time before a systematic study of the kind reported here can be made.

To summarize quickly: giant resonances consistently have \bar{N}_e around 0.5 or smaller. In low-energy peaks \bar{N}_e is more varied, and changes with neutron number in ways that depend both on the isotopic chain and on multipolarity. Strongly excited low-energy states near the drip line are sometimes scattering states but not always.

ACKNOWLEDGMENTS

This work was funded in part by the U.S. Department of Energy under grant DE-FG02-97ER41019. We thank W. Nazarewicz for useful discussion and the National Center for Computational Sciences at Oak Ridge National Laboratory, Information Technology Services at University of North Carolina at Chapel Hill, and the National Energy Research Scientific Computing Center at Lawrence Berkeley National Laboratory for the use of their computers. Parts of this research were done when one of us (J.T.) was at RIKEN.

-
- [1] M. Zinser, F. Humbert, and T. Nilsson *et al.*, Nucl. Phys. **A619**, 151 (1997).
 - [2] R. Palit, P. Adrich, and T. Aumann *et al.*, Phys. Rev. C **68**, 034318 (2003).
 - [3] T. Nakamura, N. Fukuda, and T. Kobayashi *et al.*, Phys. Rev. Lett. **83**, 1112 (1999).
 - [4] E. Tryggestad, T. Baumann, and P. Heckman *et al.*, Phys. Rev. C **67**, 064309 (2003).
 - [5] T. Hartmann, M. Babilon, S. Kamedzhiev, E. Litvinova, D. Savran, S. Volz, and A. Zilges, Phys. Rev. Lett. **93**, 192501 (2004).
 - [6] P. Adrich, A. Klimkiewicz, and M. Fallot *et al.*, Phys. Rev. Lett. **95**, 132501 (2005).
 - [7] F. Catara, C. H. Dasso, and A. Vitturi, Nucl. Phys. **A602**, 181 (1996).
 - [8] I. Hamamoto, H. Sagawa, and X. Z. Zhang, Phys. Rev. C **53**, 765 (1996).
 - [9] N. Paar, P. Ring, T. Nikšić, and D. Vretenar, Phys. Rev. C **67**, 034312 (2003).
 - [10] D. Sarchi, P. F. Bortignon, and G. Colò, Phys. Lett. **B601**, 27 (2004).
 - [11] S. Goriely, E. Khan, and M. Samyn, Nucl. Phys. **A739**, 331 (2004).
 - [12] J. Terasaki and J. Engel, Phys. Rev. C **74**, 044301 (2006).
 - [13] N. Tsoneva, H. Lenske, and Ch. Stoyanov, Phys. Lett. **B586**, 213 (2004).
 - [14] G. Tertychny, V. Tselyaev, and S. Kamedzhiev *et al.*, Nucl. Phys. **A788**, 159c (2007).
 - [15] E. Litvinova, P. Ring, and D. Vretenar, Phys. Lett. **B647**, 111 (2007).
 - [16] Y. Suzuki, K. Ikeda, and H. Sato, Prog. Theor. Phys. **83**, 180 (1990).
 - [17] A. Messiah, *Quantum Mechanics* (North Holland, Amsterdam, 1961).
 - [18] F. Calvayrac, P.-G. Reinhard, E. Suraud *et al.*, Phys. Rep. **337**, 493 (2000).
 - [19] J. Terasaki, J. Engel, M. Bender, J. Dobaczewski, W. Nazarewicz, and M. Stoitsov, Phys. Rev. C **71**, 034310 (2005).
 - [20] M. Matsuo, K. Mizuyama, and Y. Serizawa, Phys. Rev. C **71**, 064326 (2005).